FINITE ELEMENT ANALYSIS OF WINDING NIP MECHANICS

By

B. K. Kandadai[1] and J. K. Good
Oklahoma State University
USA

ABSTRACT

Wound-on-Tension (WOT) is the tension in the outermost layer of a winding roll that is created due to the incoming web tension and the tension induced by the nip roller called Nip-Induced-Tension (NIT). This paper presents the analysis of the contact mechanics between the nip roller, incoming web layer and the winding roll and explains the development of wound-on-tension in a winding process. In order to understand the contact mechanics an explicit finite element formulation is employed. The results show that the surface tractions that exist in the top and the bottom surfaces of the incoming layer underneath the nip roller give rise to a net traction. The sum of the incoming web tension and the total traction which is calculated as the integrated value of the net traction over the contact width produces the wound-on-tension. The numerical results show that the NIT is equivalent in both center and surface winding.

NOMENCLATURE

$A(t)$	Amplitude ratio as a function of time 't'
A_s, A_f	Starting, Final amplitude values respectively
b_1, b_2	Linear, Bulk viscosity coefficients
D	Stiffness Matrix
E_{11}, E_{22}, E_{33}	Modulus in principal direction
G_{12}	Shear Modulus
K_1, K_2	Pfeiffer's constants
N, NIT	Nip load, Nip-Induced-Tension
$p(x)$, P	Pressure acting on the surface of a given layer, Pressure
P_{top}, P_{bot}	Pressure acting on top and bottom surfaces respectively
$q_{top}(x)$, $q_{bot}(x)$	Top and Bottom surface tractions acting on a given layer

[1] B. K. Kandadai works as a Mechanical Engineer at Kimberly-Clark Corporation.

$q_{net}(x)$, Q	Net traction, Total traction
t, t_s, t_f	Time, Starting, Final time values respectively
T_{in}, WOT, NIT	Web tension, Wound-on-Tension, Nipt-Induced-Tension
x/a, a	Normalized contact width, contact width
ϵ, ε_2	Strain vector, Compressive Strain
$\mu_{N/w}$, $\mu_{w/w}$, $\mu_{c/w}$	Kinetic coefficient of friction between nip/web, web/web, core/web
ν_{12}, ν_{13}, ν_{23}	Poisson's ratio (v_{12} – '1' loading direction, '2' deformation direction)
$\xi(t)$	Ratio of time difference as a function of time 't'
σ_{11}, σ_{22}, σ_{33}	Principal stresses
τ_{12}, τ_{crit}	Shear stress, Critical shear stress
ω_c, ω_N	Core and Nip roller angular velocity

INTRODUCTON

In the field of winding and web handling, study of the effect of a nip roller on the wound rolls began in the late 1960's. Past studies typically fall either under theoretical or experimental nip mechanics. In this paper only relevant contribution to the field of theoretical nip mechanics have been reviewed. Contributions in experimental nip mechanics have been reviewed in Kandadai and Good [1].

Good and Wu [2] were the first to use finite element methods to understand the contact mechanics of a rolling nip and a stack of sheets. They observed that the presence of an elongating machine direction strain as a result of a compressive Hertzian-like contact stress causes NIT when the layers in the back of the nip are constrained. They showed that the maximum nip induced tension is equal to the coefficient of friction multiplied by the nip load. However their model did not account for the contact mechanics between the sheets. Welp and Gueldenberg [3] proposed a coupled contact mechanical model to understand the nip mechanics however their assumptions of stick and slip in the contact zone were incorrect and the contact conditions were not modeled adequately. Jorkama and von Hertzen [4] developed a contact mechanical model based on Fourier-series solutions derived for a linear orthotropic half space, nip roller and the incoming web. Their results show that the contact tractions due to the slippage between the nip/web and the web/wound roll interfaces results in the NIT. One of the shortcomings of their model is the inability of the model to accommodate the slippage between layers within the wound roll as the wound roll was assumed to be a solid cylindrical body. Also, their results were compared to the WOT values measured using the load cell method which can be an interfering method [5].

Good [6] came up with a closed-form solution for NIT based on the assumptions of slip and stick zones in the contact zone. He defined traction capacity (the ability to resist slip) as an integral sum of the value of coefficient of friction multiplied by the normal pressure at any point in the contact zone. The strain in the machine direction was assumed to be caused due to the Poisson effect caused by the normal stress similar to that given by Johnson [7]. The NIT was defined as the value that exists at the intersection of the traction capacity and MD stress curve and this model was verified with experimental measurements. Though both Good's and Jorkama's theories are different, it is apparent from their theories that NIT is limited by the frictional forces between the layers. Ärölä and von Hertzen [8] studied the rolling contact problem of a cylindrical drum on a stack of paper sheets using the finite element method. They observed that the net contact traction in the top layer gave rise to the NIT which was similar to what Jorkama observed.

However their observations of traction behavior in the bottom surface of the top layer were incorrect.

Kandadai and Good [9] used an explicit finite element formulation to model a center winding process with and without a nip roller. Although their model accounted for the overall effect of the nip roller, the mesh density used was too coarse to understand the nip mechanics since it was unknown if solutions were possible with higher mesh densitite to model the contact of a nip with a winding roll that would solve in reasonable amount of time. This paper addresses the above using a model that has higher mesh density required to model the nip contact mechanics and describes how the WOT is developed in a winding process without imposing many of the limiting assumptions used by Good, Jorkama and Arola.

WOUND ROLL FINITE ELEMENT MODEL

In a typical winding process, during the start of winding process, the incoming pre-tensioned layer is fastened to the core and layers are then wound on top of the core. Depending on the type of the winding process, winding is accomplished by providing torque to the core shaft (center winding) or to the nip roller (surface winding). The FE model that is used to analyze the development of WOT in a center and surface winding process is described below.

Model Set Up

The model is set up such that it resembles a real winding process closely. Consider an initial configuration in which the incoming web layer is tied to the rigid core as shown in Figure 1a. The core and the nip roller are modeled as rigid cylindrical bodies. The web is modeled as an elastic layer of constant thickness. Winding is then accomplished in different steps that are a function of time in ABAQUS/Explicit® (a commercial FE program).

In the first time step, a known value of load (distributed load 'T_w' at the end of the sheet) is prescribed at the left end of the sheet. This simulates the web tension in the incoming sheet as shown in Figure 1b. In this time step, the center of rotation of the core is fixed in all degrees of freedom while the nip roller is pinned. In the second time step, the nip roller contacts the incoming web under a prescribed nip load 'N'. In this time step, the boundary conditions are modified such that the center of rotation of the nip roller is fixed only in the horizontal degree of freedom and is free to move vertically as well as rotate about its axis as shown in Figure 1c. This facilitates the application of nip load vertically. In the third step, winding of the roll is accomplished by prescribing an angular velocity to the rigid core (in center winding) and to the rigid nip roller (in surface winding) as shown in Figure 1d. Also, the rotational constraint on the rigid core is removed during this step to facilitate the winding process. The model properties are summarized in Table. 1. The winding problem is analyzed in plane strain conditions as a quasi-static problem so that mass-related effects are negligible. The core and the nip roller are modeled as rigid analytical surfaces. The web is modeled as an elastic solid using four-noded isoparametric quadrilateral elements in reduced integration mode [10].

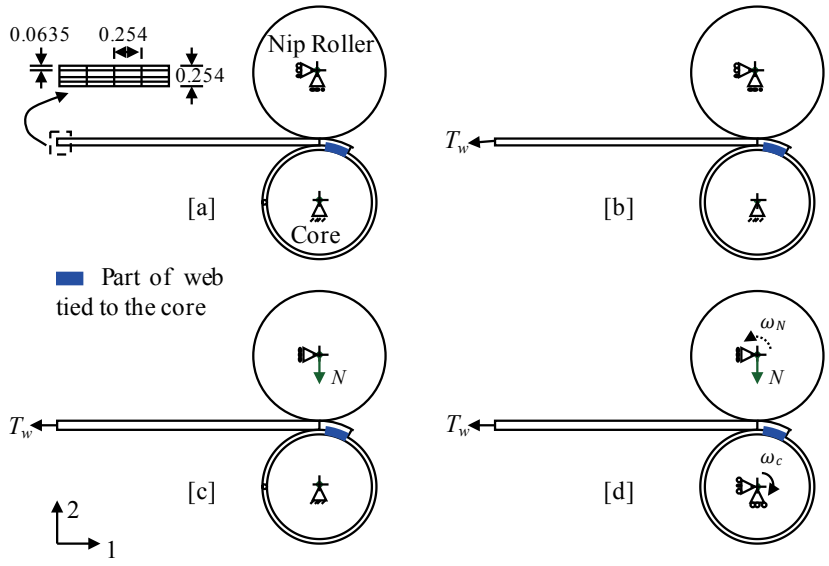

Figure 1 – Schematic representation of the FE model set up
(Dimensions expressed in cm)

Property	Value
Web length	140.6 cm
Web thickness	0.0254 cm
Rigid core diameter	8.89 cm
Rigid nip roller diameter	10.16 cm
Angular velocity (ω_c , ω_N)	3, 3.53 rad/sec
Coefficient of friction ($\mu_{N/w}$, $\mu_{w/w}$, $\mu_{c/w}$)	0.18, 0.16, 0.18
Web tension (T_{in})	5.25 N/cm
Nip load (N)	43.8, 58.4, 87.6, 109.4 N/cm

Table 1 – Winding model properties.

In order to reduce mass-related effects, the load and velocity boundary conditions are ramped to their final values smoothly. Physical damping was not used in the model. The default values for numerical damping used in ABAQUS/Explicit® were left unchanged. The default values for linear 'b_1' and quadratic 'b_2' bulk viscosity coefficients in ABAQUS/Explicit® were 0.06 and 1.2 respectively. Since increasing or decreasing the default damping factors by a factor of 10 did not change the solution appreciably (less than 1% change) the default values were used. Also, a mass scaling factor of 300 was used to reduce the total computational time while ensuring that accuracy is not sacrificed. A typical wound roll is made up of many layers (often thousands). However winding an entire roll in ABAQUS/Explicit® is computationally expensive. In order to get a basic understanding of the nip mechanics and the development of WOT in a winding process the model was run till 5 layers are wound onto a rigid core. The winding model consists of 17,706 nodes and 13,279 elements with 35,414 degrees of freedom. The analysis takes on an average of 240 hours to complete on desktop computers with average processing

capabilities equivalent to that of an Intel Pentium IV® 3.0 GHz processor with 1 Gigabyte of RAM.

Material Properties and Constitutive Relationship

Most materials in web form like paper, film are anisotropic due to the directional orientation imparted during the forming processes. In this paper a 1000 gage (0.0254 cm/0.01 in) PET (Polyethylene terapthalate) film with a density of 1.66 g/cm^3 was used to model the web layer. The anisotropy of this PET film is characterized below. The machine direction (E_{11}) and cross-machine direction (E_{33}) modulus of the film were measured at 4895 MPa and 5102 MPa respectively. The modulus in the radial direction (E_{22}) called as the radial modulus varies non-linearly with strain. Pfeiffer [11] showed this behavior in stacks of different grades of paper. Pfeiffer approximated the behavior of compressive strain for a web stack using equation (2). 'K_2' is referred to as the springiness factor. The advantage of using this type of curve-fit for radial modulus is the ability to compare different webs when values of 'K_2' are known. The radial modulus is estimated as the slope of the pressure-strain curve as given in equation (2). Compression tests were conducted on a 2.54 cm (one inch) high stack of PET webs that were cut into 15.2 X 15.2 cm^2 coupons and stacked on top of each other. The experimental stress-strain behavior along with Pfeiffer-type curve fit is shown in Figure. 2. However, in order to keep the computational time to a reasonable limit and to get a basic understanding of the nip mechanics, E_{22} is set to a constant value of 16.3 MPa and is estimated based on an average pressure corresponding to a nip load of 43.8 N/cm [12].

$$P = K_1\left[e^{K_2\varepsilon_2} - 1\right]; \quad E_{22}(P) = \frac{dP}{d\varepsilon_2} = K_2\left[K_1 + P\right] \qquad \{1\}$$

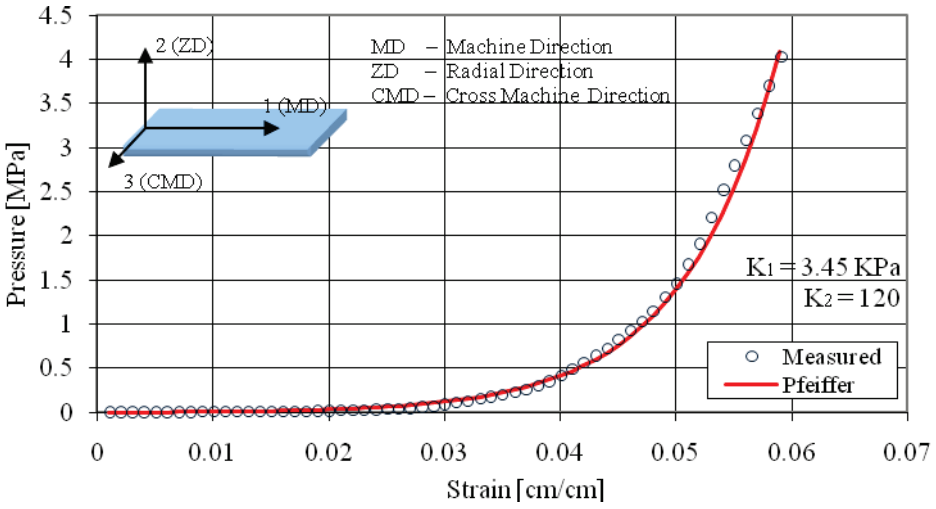

Figure 2 – Behavior of a stack of PET webs under compressive loading.

From various references [13-15], the in-plane Poisson's ratio 'ν_{13}' was found to be between 0.29 and 0.39 and a value of 0.36 was chosen for this analysis. Generally, the

value of out-of-plane Poisson's ratio 'v_{12}' is assumed to be a constant for film webs and is in the range of 0.3-0.4. In this paper a value of 0.3 was for v_{12}. G_{12} was estimated using equation (3) which was originally developed by St. Venant's and later used by Cheng and Cheng [16]. For the PET film used in this research, a value of 16.3 MPa was obtained using equation (3) based on E_r calculated using an average nip pressure for a nip load of 43.8 N/cm. The material orientation is shown in Figure.2 and the compliance matrix is given in equation (4). All the material constants are summarized in Table. 2. Note that the values of G_{13}, G_{23} and v_{23} do not affect the 2-D plane strain equations.

$$G_{12} = \frac{E_{11}E_{22}}{E_{11}\left(1+\nu_{21}\right)+E_{22}\left(1+\nu_{12}\right)} \qquad \{2\}$$

Material Constant	Value
E_{11}, E_{22}, E_{33}	4895, 16.3, 5102 MPa
ν_{13}, ν_{12}	0.36, 0.3
G_{12}	16.3 MPa

Table 2 – Material properties of 1000 gage PET film.

$$\sigma = D:\in; \quad \begin{Bmatrix} \varepsilon_{11} \\ \varepsilon_{22} \\ \varepsilon_{33} \\ \gamma_{12} \end{Bmatrix} = \begin{bmatrix} \frac{1}{E_{11}} & -\frac{\nu_{21}}{E_{22}} & -\frac{\nu_{31}}{E_{33}} & 0 \\ -\frac{\nu_{12}}{E_{11}} & \frac{1}{E_{22}} & -\frac{\nu_{32}}{E_{33}} & 0 \\ -\frac{\nu_{13}}{E_{11}} & -\frac{\nu_{23}}{E_{22}} & \frac{1}{E_{33}} & 0 \\ 0 & 0 & 0 & \frac{1}{G_{12}} \end{bmatrix} \begin{Bmatrix} \sigma_{11} \\ \sigma_{22} \\ \sigma_{33} \\ \tau_{12} \end{Bmatrix} \qquad \{3\}$$

Surface Interaction Behavior

At the start of the winding process, the bottom surface of the incoming web layer contacts the rigid core. After one revolution of the core, the bottom surface of the incoming web layer contacts the top surface of the winding roll. Also, in center or surface winding the top surface of the incoming web layer contacts the rigid nip surface. Thus, one of the challenges in modeling a winding process using an explicit FE method is to accurately model the surface interactions. This is accomplished by modeling the contact pairs using a kinematic predictor-corrector contact algorithm [17] to strictly enforce the contact constraints that allows for no nodal penetrations. The friction between all contacting surfaces is modeled using the Coulomb's friction law with a constant coefficient of friction. The Coulomb friction model relates the maximum allowable frictional (shear) stress across an interface to the contact pressure between the contacting bodies. In Coulomb friction model, two contacting surfaces can carry shear stresses up to a certain magnitude across their interface prior to sliding relative to one another; this state is known as sticking. The Coulomb friction model defines this critical shear stress 'τ_{crit}' as the stress at which sliding of the surfaces starts at a fraction of the contact pressure '$p(x)$' between the surfaces. The stick/slip calculations determine when a point in a contact

region moves from sticking to slipping or from slipping to sticking as given in equation (5).

$$\begin{aligned} \tau_{crit} &= \mu\, p(x) \quad \rightarrow Slip \\ \tau_{crit} &< \mu\, p(x) \quad \rightarrow Stick \end{aligned} \qquad \{4\}$$

Based on ASTM measurements, the results show that the values of the kinetic coefficient of friction '$\mu_{N/w}$' and '$\mu_{w/w}$' are 0.18 and 0.22 respectively. Kandadai [11] showed that coefficient of friction value inferred from the flat bed experimental measurements of NIT closely represented the frictional conditions that exists in rolling contact conditions in a winding process compared to ASTM measurements. For the PET used in this research, Kandadai [12] measured a value of 0.16 for '$\mu_{w/w}$' and this value will be used in the model.

FE MODEL RESULTS: CENTER AND SURFACE WINDING

The development of WOT and the contact mechanics in a winding process using a five layer FE model is discussed below. A schematic of the winding process and the notation for the analysis of results is shown in Figure. 3. Observe that the layer on top of the core is represented as 'layer 5' and the layer in contact with the nip roll is represented as 'layer 1'. Consider a winding process and the forces of interaction between the incoming web layer, the nip roller and the winding roll as shown in Figure. 3. In a winding process, the incoming layer becomes a part of the winding roll past the nip. Due to frictional rolling contact between the surfaces involved and the boundary conditions of the winding process, surface tractions arise at the top and bottom surfaces. These surface tractions give rise to a net traction calculated as the sum of the top and bottom surface tractions of the incoming web layer. This net traction varies through the contact zone and is dependent on the conditions of slip and stick in the top and bottom surfaces within the rolling contact zone. The integrated value of the net traction is commonly referred to as the total traction and is calculated as given in equation (6). When the incoming layer does not wrap the nip roller (like shown in the figure), based on the equilibrium of forces, the total tension 'T_{out}' in the web at the exit zone of the nip (also referred to as WOT) can be calculated as shown in equation (7) if the total traction 'Q' and the incoming web tension 'T_{in}' are known.

$$Q = \int_{-a}^{a} q_{net}(x)dx \quad \text{where } q_{net}(x) = q_{top}(x) + q_{bot}(x) \qquad \{5\}$$

$$T_{out} = T_{in} + \int_{-a}^{a} \left[q_{top}(x) + q_{bot}(x) \right] dx \qquad \{6\}$$

Consider a center winding process where in the web tension is 5.25 N/cm and nip load is 43.8 N/cm. As the incoming layer goes through the nip and becomes part of the winding roll both bending and membrane stresses are created in the outer layer. The behavior of the machine direction stresses (σ_{11}) stresses after five layers are wound as a function of the total length of the web material is shown in Figure. 4. In the figure, the region wherein the total web length is less than 3 inches (free span), the web is under the prescribed value of web tension (5.25 N/cm). Beyond this region, the web becomes part of the wound roll. The top and bottom surface σ_{11} stresses include both the bending and

membrane component of the tension. The WOT is the membrane component of the σ_{11} stress and is calculated by averaging the top and the bottom surface stresses. As the incoming web passes through the nip, the overall tension increases due to the nip action and remains constant in the outermost layer.

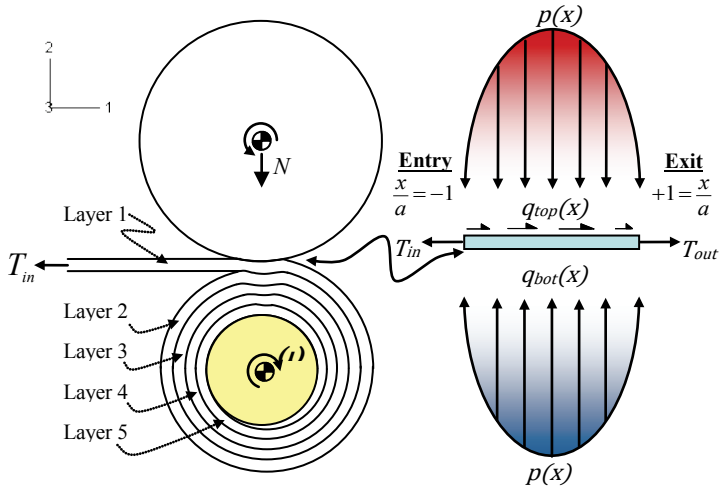

Figure 3 – Schematic representation of the forces acting in the nip contact zone

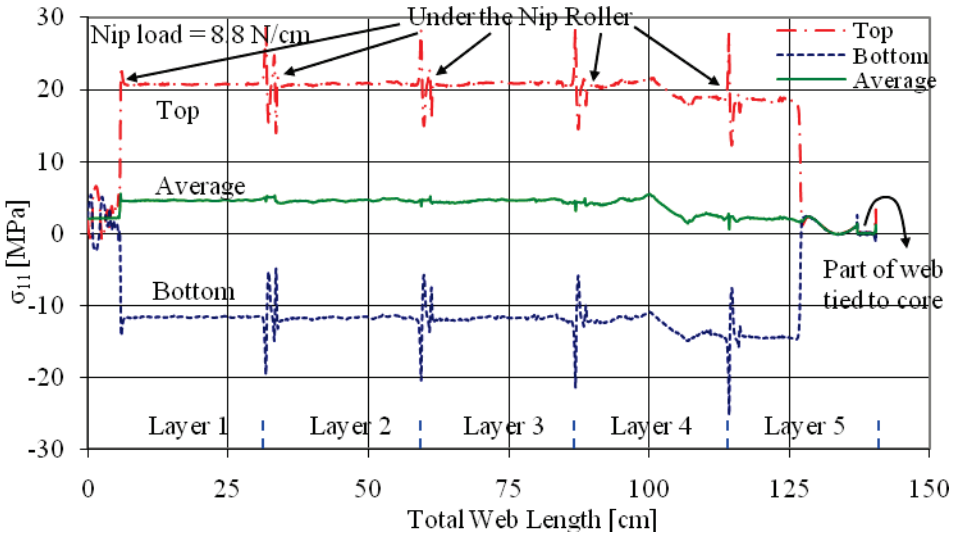

Figure 4 – Behavior of the top, bottom and average 'σ_{11}' stresses in a center wound roll at T_{in}=5.25 N/cm and a nip load of 43.8 N/cm.

In the figure, in each layer, two peaks can be observed. One of the peaks is due to the stresses caused as a result of stress concentration caused by the roll start up as shown in Figure. 5. The other is due to the contact stresses and bending of the web due to the nip roller in the contact zone. The average σ_{11} stress in layers 2 and 3 do not change appreciably from WOT. This behavior is very different compared to what was observed by Arola and von Hertzen [8]. They found that the layers underneath the first layer were at much lower tension or in compression. In their case the model was set up to understand the contact mechanics between a rolling nip roller and a stack of web layers constrained at one end. However in the winding model, once the incoming layer becomes part of the winding roll it gets constrained by the layers that are added on top of it. Addition of each layer causes significant radial pressure in the layers beneath the outermost layer that inhibits slip between the layers and due to this the WOT is constant through the outermost layer.

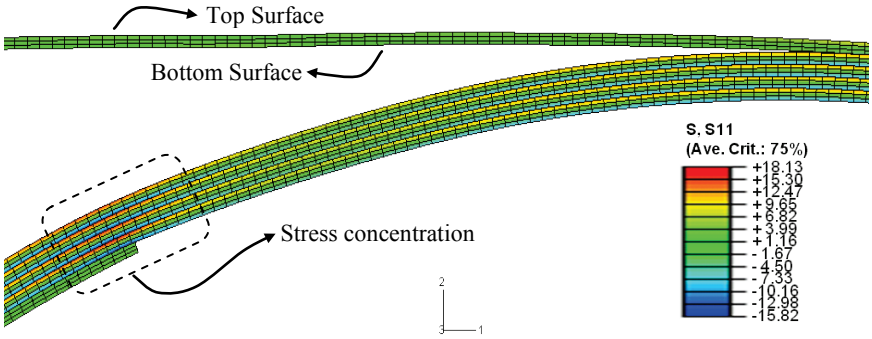

Figure 5 – Effect of the start up of the wound roll on the bending stresses.

The behavior of the surface tractions and 'σ_{11}' stresses in each layer underneath the nip roller is shown in Figure. 6. In the contact zone, the contact pressure varies from zero at one end to a maximum value at the center of nip contact and goes back down to zero at the other end. Based on equation (11) the maximum shear stress can be calculated for the top and bottom surface at discrete points and when plotted over the normalized contact width (x/a) the stresses form an envelope ($\pm\mu p(x)$ boundary) as shown in Figure. 6. When the top and bottom surface tractions are also plotted in the same figure, regions of stick and slip can be identified. The surface is under slip when the surface traction at a given node falls on the $\pm\mu p(x)$ envelope. The surface is in stick condition when the surface traction at a given node falls within the $\pm\mu p(x)$ envelope. Under slip condition surfaces travel at different speeds, while in stick the relative velocity between them is zero.

In the topmost layer, the top surface tractions exhibit three distinct regions; slip at both ends of contact and a large stick zone in the middle. This indicates that the top surface of the incoming sheet moves faster at the edges of contact zone and at the same speed as the nip roller surface in the middle of the contact zone. The bottom surface is under micro-slip and exhibits five distinct regions. The edges of contact are under slip and although the middle of the contact slips, it slips in a direction opposite to the slip at the ends. Between each of these slip zone, a stick zone exists. The behavior of the surface tractions indicate that the bottom surface of the topmost layer moves slower compared to the top surface of the second layer at the edges of the contact. In the two intermediate stick zones, the surface velocities of the bottom surface of the topmost layer and the top

surface of the second layer are equal. In the middle slip zone, the direction of the surface traction is opposite compared to the ones at the edges. This indicates that the velocity of the bottom surface of the topmost layer in this region is faster than the top surface of the second layer.

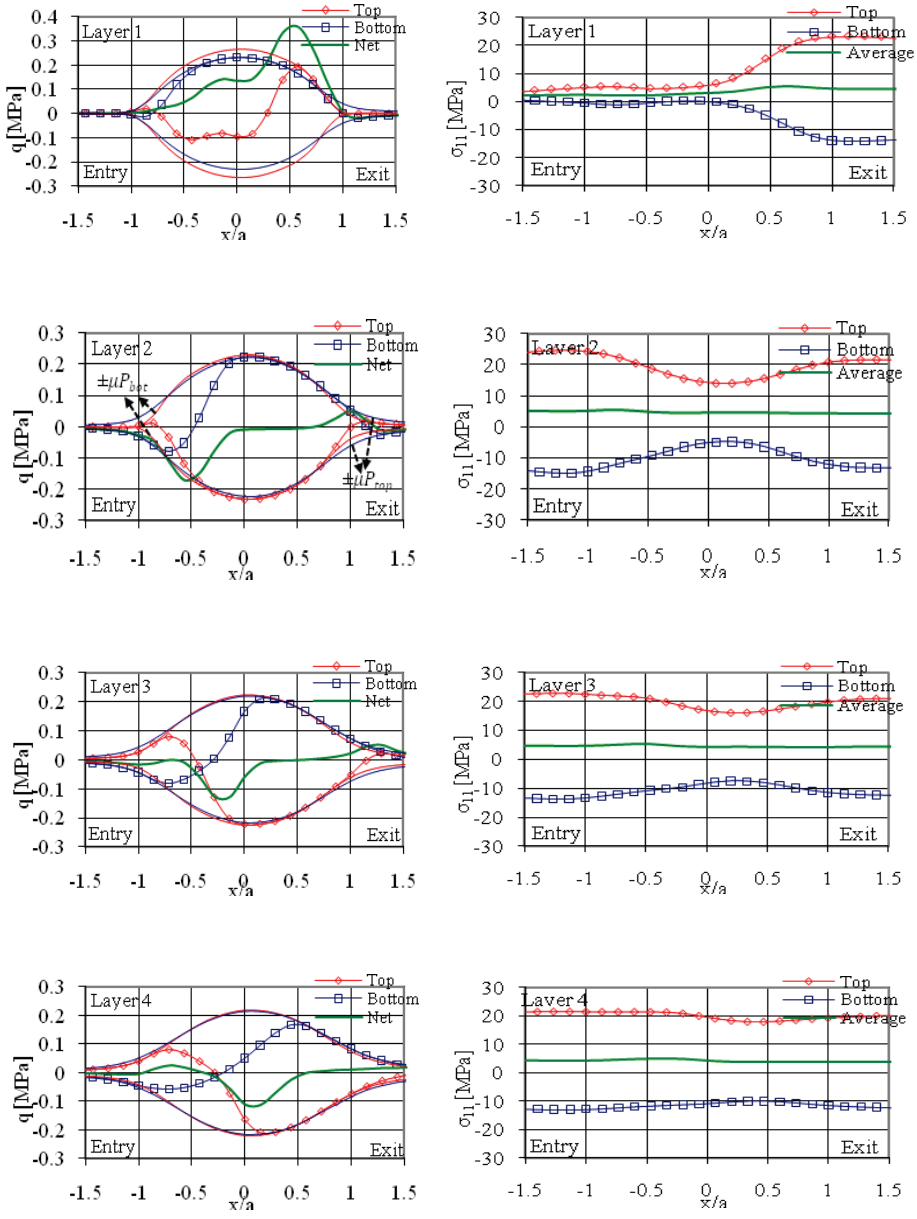

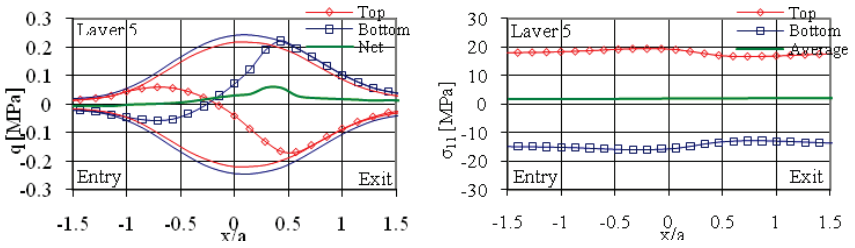

Figure 6 – Behavior of the surface tractions and the 'σ_{11}' stresses in the nip contact zone in a center winding process with an undriven nip roller at a web tension of 5.25 N/cm and a nip load of 43.8 N/cm.

An unbalanced net traction that is calculated as the sum of the top and bottom surface tractions exists in the topmost layer. The total traction can be calculated by adding the net traction values calculated at discrete points in the contact zone. The sum of the web tension and the total traction becomes the WOT as explained in section 2.4. and was found to be equal to the 'σ_{11}' stress at the exit of the contact zone as shown in Figure. 6. The qualitative behavior of the surface traction in layers below the topmost layer is similar to the behavior observed in the topmost layer. In the case of surface winding, the behavior of the surface tractions and the 'σ_{11}' stresses are similar. However, the final value of the WOT differs by the value of web tension as discussed in the following section.

The effect of nip load on the WOT in center and surface winding is shown in Figure 7. In the figure, the WOT is expressed in units of Pli. It is calculated by multiplying the average value of 'σ_{11}' stresses (membrane only) in the outermost layer with the web thickness. As the nip load increases, the WOT increases linearly in both center and surface winding. At the highest nip load, the WOT begins to taper off in center winding. Note that the difference between WOT in center and surface winding at different nip loads is equivalent to web tension. Although the underlying contact mechanics remain the same between center and surface winding, the behavior of the surface traction within the contact zone is entirely different in each case.

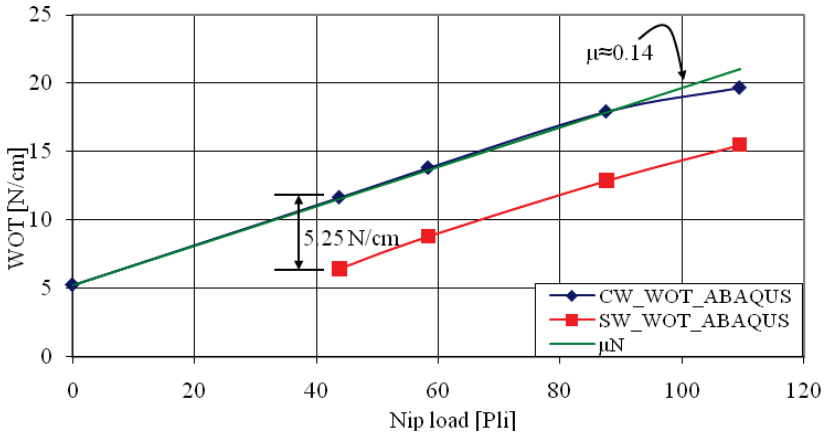

Figure 7 – Effect of nip load on WOT in center and surface winding

The behavior of top and bottom surface tractions in center and surface winding at different nip loads is shown in Figure. 8. The primary difference lies in the behavior of the top surface tractions. When the top surface traction is integrated in center winding the net value is zero as the nip does not act as a driving roll in the winding process. This indicates that all of the web tension goes into WOT in center winding. In surface winding, the integrated value of top surface traction is almost equivalent to web tension. This indicates that a significant part of the top surface traction in the outermost layer (incoming web) in surface winding is expended in overcoming the web tension and in driving the winding roll. This indicates that the WOT in surface winding is almost independent of web tension.

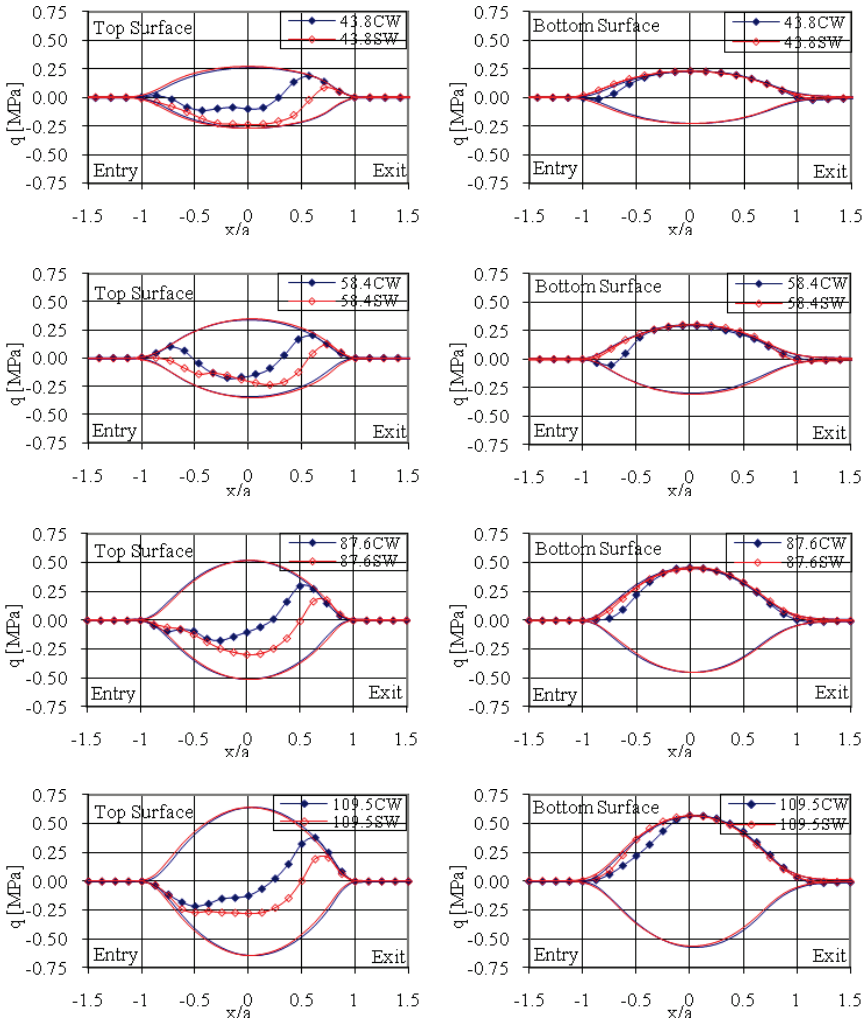

Figure 8 – Comparison of top and bottom surface tractions between center and surface winding process

The net tractions in center and surface winding are compared for different nip loads in Figure. 9. In both center and surface winding, as the nip load increases, the contact pressure increases and as a result the traction limits increase. Given a winding process, the top surface traction exhibits similar behavior at all nip loads as shown in Figure. 8. In center winding, the bottom surface is under micro-slip at all nip loads. However the stick zone near the entry grows as the nip load increases. As the stick zone increases in the bottom surface, the total traction calculated by integrating the net traction through the contact width decreases from the maximum possible value of μN. Although this behavior is similar in surface winding, the size of the stick zone is much smaller at high nip loads as shown in Figure. 8.

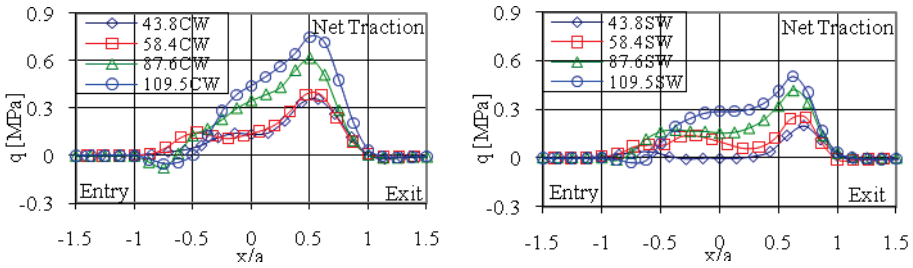

Figure 9 – Comparison of top, bottom and net surface tractions between center and surface winding process at different nip loads.

In center winding, when the incoming web does not wrap the nip roller, the integrated value of the top surface traction in the contact zone is zero. This indicates that all of the web tension in center winding goes into WOT. In surface winding, when the top surface traction is integrated through the contact zone it is equivalent to the incoming web tension but acts in the opposite direction. Hence in surface winding, the integrated value of top surface traction must compensate for the incoming tension so that winding can be accomplished. Thus all the WOT produced in surface winding is nip induced and is largely independent of the web tension. The NIT in center and surface winding is shown in Figure. 10. The data in the figure indicates that the NIT is similar in center and surface winding at a given nip load and hence, independent of the winding process. This is consistent with the observations of Good et al. [5] in center and surface wound rolls of newsprint.

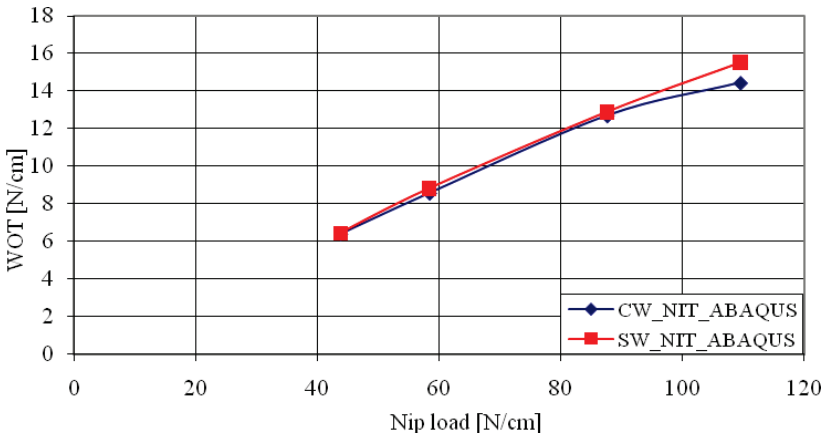

Figure 10 – Comparison of NIT in center and surface winding processes

CONCLUSIONS

An explicit FE method has been used to model the development of WOT in center and surface winding method. The results of the analysis shows that the surface traction behavior in the nip contact zone governs the WOT development. Distinct behavior is observed in the top and bottom surfaces that gives rise to WOT. The top surface tractions exhibit three distinct regions. At the edges of the contact, the surface is under slip and the surface velocity of the web is higher than the velocity of the drum. In the middle of the contact, the top surface is under stick and in this zone, the surface velocities are equal. The bottom surface of the topmost layer is under micro-slip and exhibits five distinct regions. The surface is under slip at the edges of contact and in these zones, the bottom surface of the web moves slower than the top surface of the second layer. In the middle of the contact, another slip zone exists and in this zone the bottom surface moves faster than the top surface of the second layer. Between these slip zones, two intermediate stick zones exist wherein the surface velocities are equal. This micro-slip behavior in the bottom surface dictates the amount of NIT developed during the winding process.

The results show that the sum of the incoming web tension and the integrated value of the net traction which is calculated as the sum of top and bottom surface tractions in the contact zone is equivalent to the WOT. In both center and surface winding, at low nip loads, the numerical results show that the NIT is approximately equal to '$\mu_{Web/Web}.N$'. At high nip loads, the NIT starts to taper off and decreases from the maximum possible value of '$\mu_{Web/Web}.N$'. In surface winding, the numerical results show that the integrated value of the top surface traction is equal to the web tension so long as winding is possible. The numerical results show that the NIT is similar in both center and surface winding for a given level of nip load. This is consistent with the observations of Good et al [5].

REFERENCES

1. Kandadai, B. K. and Good, J.K., "Measurement of Nip Induced Tension and Contact Stresses," Proceedings of the Tenth International Conference on Web Handling, Web Handling Research Center, Oklahoma State University, Stillwater, Oklahoma, 2009.

2. Good, J. K. and Wu. Z., "The Mechanism of Nip Induced Tension in Wound Rolls," Journal of Applied Mechanics, Transactions of ASME, Vol. 60, 1993, pp. 942-947.
3. Welp. E. G. and Gueldenberg. B., "Analysis of the Kinematic and Dynamic Process during Winding based on a Systematology of Models for Winding Mechanics," Proceedings of the Fourth International Conference on Web Handling, Web Handling Research Center, Oklahoma State University, Stillwater, Oklahoma, 1997, pp. 71-89.
4. Jorkama. M. and von Hertzen. R., "The Mechanism of Nip Induced Tension in Winding," Journal of Pulp and Paper Science, Vol. 28, 2002, pp. 280-284.
5. Good, J. K, Hartwig. J, and Markum. R., "A Comparison of Center and Surface Winding Using the Wound-In-Tension Method," Proceedings of the Fifth International Conference on Web Handling, Web Handling Research Center, Oklahoma State University, Stillwater, Oklahoma, 1999, pp. 87-104.
6. Good. J. K., "Modeling Nip Induced Tension in Wound Rolls," Proceedings of the Sixth International Conference on Web Handling, Web Handling Research Center, Oklahoma State University, Stillwater, Oklahoma, 2001, pp. 103-122.
7. Johnson. K. L., Contact Mechanics, Cambridge University Press, 1985.
8. Arola. K. and von Hertzen. R., "Development of Sheet Tension under a Rolling Nip on a Paper Stack," International Journal of Mechanical Sciences, Vol. 47, 2005, pp. 110-133.
9. Kandadai, B. K. and Good, J. K., "Modeling Wound Rolls using Explicit Finite Element Methods", Proceedings of the Ninth Interntational Conference on Web Handling, Web Handling Research Center, Oklahoma State University, Stillwater, Oklahoma, 2007.
10. ABAQUS Inc., ABAQUS User's Manual, 2005.
11. Pfeiffer. J. D., "Measurement of the K2 Factor for Paper," TAPPI Journal, 1980, pp. 139-141.
12. Kandadai, B. K., "The Development of Wound-on-Tension in Webs Wound into Rolls," PhD Dissertation, Oklahoma State University, 2006.
13. Feng, R. and Farris. J. R., "Linear Thermoelastic Characterization of Anisotropic Poly(ethylene terephthalate) Films," Journal of Applied Polymer Science, Vol. 86, 2001, pp. 1937-1947.
14. Okabe. Y, Takeda. N, Yanaka. M., and Tsukahara. Y., "Determination of the Orthotropic Elastic Constants of Thin PET Film by an Ultrasonic Micro-Spectrometer," IEEE Transactions on Ultrasonics, Ferroelectrics, and Frequency Control, Vol. 46, 1999, pp. 1269-1275.
15. Zhang. S. L. and Li. J. C. M., "Anisotropic Elastic Moduli and Poisson's Ratios of a Poly(ethylene terephthalate) Film," Journal of Polymer Science: Part B: Polymer Physics, Vol. 42, 2004, pp. 260-266.
16. Cheng. S. and Cheng. C. C., "Relation between E, ν, G and Invariants of the Elastic Coefficients for an Orthotropic Body," The Winter Annual Meeting of the American Society of Mechanical Engineers, Dallas, Texas, Applied Mechanics Division and the Materials Division, ASME, Vol. 112,1990, pp. 63-65.
17. ABAQUS Inc., ABAQUS Theory Manual, 2005.

	Finite Element Analysis of Winding Nip Mechanics	**B. K. Kandadai & J. K. Good**, Oklahoma State University, USA

Name & Affiliation	**Question**
Bob Lucas, Winder Science	From a modeling point of view, you are saying considerable CPU time is required to complete the simulations. Is it possible that those elements that are far removed from the nip could be considered dormant elements? Could the active degrees of freedom be reduced at any particular time?
Name & Affiliation	**Answer**
Balaji Kandadai, Kimberly-Clark Corporation	The reason we are modeling the entire roll is we wanted to simulate how the cushion effect resulting from layers wound previously underneath the current outer layer affect the wound-on-tension. We in fact tried to treat the previous layers as a homogenous foundation. When I tried this, I could not get the wound-on-tension to match test results. There is a difference in treating the wound roll as a spiral wound from a continuous layer as opposed to simulating a calendaring process where you are modeling a web passing between an elastic core and a rigid nip. The wound-on-tensions computed differed from the continuous winding process.
Name & Affiliation	**Question**
Bob Lucas, Winder Science	Research conducted 30 years ago showed that often a bubble or slack region of web would form upstream of a winding nip. This was not apparent in Figure 4.
Name & Affiliation	**Answer**
Balaji Kandadai, Kimberly-Clark Corporation	I did not witness that in the model results. In my next presentation that focuses on testing I did not witness the behavior you describe either. In my simulations the web was entering the wound roll and nip at a tangent, the web did not wrap the nip or the wound roll. Dr. Good, do you want to comment on that?
Name & Affiliation	**Answer**
J. K. Good, Oklahoma State University	Balaji has assessed this correctly. If in fact, the layer was wrapping the winding roll prior to entering the nip, you would have the potential to witness the bubble Bob Lucas described. The nip induces tension in the outer lap by causing it to slip over the layer beneath. The same slippage that caused the tension to increase in the outer lap could cause a tension drop or complete loss of web tension upstream of the nip if the web first wrapped either the nip or the wound roll prior to nip entry. In the case being simulated here the web upstream of the nip is in a free span in which the tension is held constant, thus there is no opportunity for an out-of-plane deformation or bubble to exist.

Name & Affiliation	Question
Bob Lucas, Winder Science	You commented that you assumed a linear orthotropic material model. In your paper you acknowledge that the wound roll can have state dependent properties, but that is not included here.
Name & Affiliation	**Answer**
Balaji Kandadai, Kimberly-Clark Corporation	That is correct. In order to incorporate state dependent material behavior, I had to write a separate subroutine that would update the web properties as a function of pressure after each time step. This caused the computation time to increase exponentially. We decided to approximate the radial modulus E_r for a given nip load at a constant value. We used a contact mechanics formulation to calculate average pressure in the nip contact zone. This formulation was developed by Dr. Good in his paper on the modeling of nip-induced-tension. This was done to decrease the computational time.